OFFICE OF NAVAL RESEARCH TECHNICAL REPORT FOR

Grant No. N00014-95-WR-20027

PR NUMBER: 96PRO-3804 - Robert J. Nowak

Technical Report #15

ELECTRIC POTENTIAL NEAR A CHARGED METAL SURFACE IN CONTACT WITH AQUEOUS ELECTROLYTE

Prepared for Publication in
J. Electroanal.Chem.
by

Michael R. Philpott
IBM Research Division, Almaden Research Center,
650 Harry Road, San Jose, CA 95120-6099
and
James N. Glosli
Lawrence Livermore National Laboratory,
University of California, Livermore, CA 94550

Abstract

The time independent electric potential due to water and a lithium ion near a charged metal surface is calculated by space and ensemble averaging of trajectories generated by a molecular dynamics simulation. Since the cation does not contact adsorb variations in the electric potential near the metal surface are due to water oriented in the electric field of the charged surface. The potential is decomposed into separate contributions from monopoles (from the ions), and dipoles, quadrupoles and octopoles (from the water molecules). At distances greater than about 0.5 nm from the electrode (2 - 3 water molecules) the potential is 'flat' with the quadrupole contributing most due to a near cancellation of the ion and water dipole components. Approaching the surface weak features are encountered due to water packing and then a big oscillation due to water oriented in a layer next to the electrode. None of these effects are described in theories that approximate water as a continuum fluid.

DISCLAIMER NOTICE

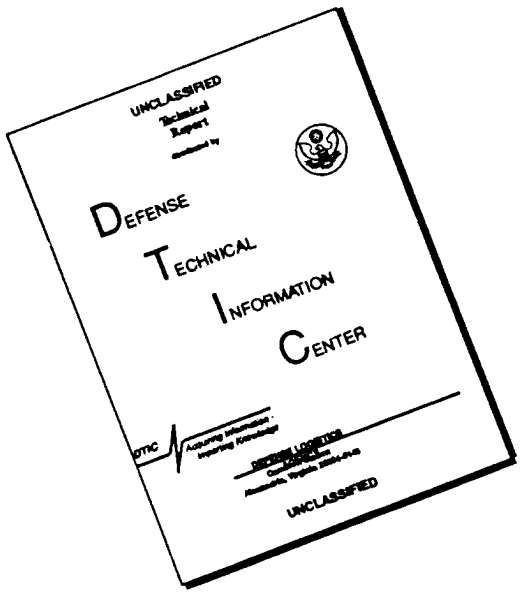

THIS DOCUMENT IS BEST QUALITY AVAILABLE. THE COPY FURNISHED TO DTIC CONTAINED A SIGNIFICANT NUMBER OF PAGES WHICH DO NOT REPRODUCE LEGIBLY.

Paper for JEAC proceedings,
Snowdonia Electrified Interfaces Meeting,
Harlech, Wales, UK July 17-22, 1995.

ELECTRIC POTENTIAL NEAR A CHARGED METAL SURFACE IN CONTACT WITH AQUEOUS ELECTROLYTE

Michael R. Philpott
IBM Almaden Research Center,
650 Harry Road, San Jose, CA 95120-6099
and
James N. Glosli
Lawrence Livermore National Laboratory,
University of California, Livermore, CA 94550

Abstract

The time independent electric potential due to water and a lithium ion near a charged metal surface is calculated by space and ensemble averaging of trajectories generated by a molecular dynamics simulation. Since the cation does not contact adsorb variations in the electric potential near the metal surface are due to water oriented in the electric field of the charged surface. The potential is decomposed into separate contributions from monopoles (from the ions), and dipoles, quadrupoles and octopoles (from the water molecules). At distances greater than about 0.5 nm from the electrode (2 - 3 water molecules) the potential is 'flat' with the quadrupole contributing most due to a near cancellation of the ion and water dipole components. Approaching the surface weak features are encountered due to water packing and then a big oscillation due to water oriented in a layer next to the electrode. None of these effects are described in theories that approximate water as a continuum fluid.

I. INTRODUCTION

In this paper we describe the calculation of the electric potential across an electrified interface using a molecular dynamics simulation performed at constant N,V,T. The simulation cell consists of one lithium ion and 157 water molecules. Lithium was chosen because it does not lose solvation and contact adsorb on the surface in the range of charge densities used (-0.288e/nm^2) in the calculation. This makes the interpretation of structure near the electrode simpler. We resolve the potential into explicit contributions from the ions and the multipole moments of the water molecules. The variation in the potentials with distance from the electrode shows structure which is related the distribution of the ion and the distribution and orientation of the water molecules. The features in the electric potential due to water are new and not found in theories that treat the solvent as a dielectric continuum. The explicit calculation of quadrupole and octopole potentials provides insight not available from theories that model the solvent as a point dipole in a sphere.

Figure 1 upper part shows schematically the electric potential of the system when water is assumed to be a simple dielectric continuum. The lower part of Figure 1 is a cartoon that provides on the molecular scale a picture of the double layer near a flat charged metal surface when there are no contact adsorbing ions. Similar pictures can be found in many textbooks and review articles. The water next to the electrode is shown as an oriented monolayer. If this first layer of water is not displaced by the cation at its distance of closest approach then the hydrated cation is two water molecules away from the surface. This is a characteristic feature of the model of Bockris, Devanathan and Müller[1-3]. In Grahame's model[4] the ions primary solvation shell can contact the electrode. The plane of closest approach of the positive ion is the outer Helmholtz plane (OHP). The diffuse region in this traditional picture starts two solvent molecules from a flat electrode surface and stretches out many nanometers into the bulk electrolyte. The Gouy and Chapman model[2] provided the first quantitative description of the diffuse layer.

This paper consists of three sections. Section II contains a brief description of model and methods. Two complementary methods were used to calculate the electric potential. In the last section III, we first briefly describe the distribution profiles for ions and water molecules obtained from the molecular dynamics simulation, and then the results of the electric potential calculations. These include the results of decomposing the potential into multipole components and a summary of the effect of varying the width of the spatial box used in making the space averages. It is shown how the water quadrupole and octopole multipole structure in the potential is washed out when the box dimension parameter approximates the size of a water molecule.

II. MODEL AND METHODS.

A. The screened electrode

Since the electrolyte solution is a conductor all charged surfaces immersed in the electrolyte are screened by displacement of ions towards the surface in such a way as to shield the bulk solution from the field of the surface charge. The simplest treatment of this phenomena is the Gouy-Chapman theory[2] which treats ions as point charges and all the solvent molecules as if they

comprised a dielectric fluid. According to this theory the concentration of monovalent ions has fallen to e^{-1} of its 'surface' value at a distance d from the electrode given by

$$d = \sqrt{\left(\frac{\varepsilon kT}{8\pi e^2 n_b} \right)} . \qquad [2.1]$$

The inverse d^{-1} is the Debye-Hückel screening constant. Here ε is the macroscopic dielectric constant of the solvent, and n_b is the concentration of the ions in the bulk. Typical values of *d* are: 3.1 nm for 0.01 M, and 0.96 nm for 0.1 M. The derivation of this formula does not hold high salt concentrations, though it can provide some guidance. For example at 0.3 M we have d = 0.55 nm which is only about twice the size of a water molecule or ion. We conclude that most of the surface charge screening takes place close to the electrode and that a simulation cell with size L = 1.862 nm should be just large enough to capture most of the physics.

B. Immersed electrode model.

The model consists of a layer of electrolyte between two walls. The gap between the walls is the simulation cell edge length L = 1.862 nm. The cell contains 157 model ST2 water molecules and one lithium ion. The cell is periodically replicated in the two dimensions xy parallel to the metal surface, but not perpendicular to the surface. The wall on the left (z = -L/2) carries no charge, it is a simple restraining wall to hold the electrolyte in place. The wall on the right (z = L/2) is the metal with the plane z = L/2 the electrostatic image plane. The charge on the metal equals the image charge of the lithium ion. The total charge of the system is zero because the water molecules are individually neutral and the ion and its electrostatic image are opposite in charge. The essential feature of the immersed electrode model is that the charge in solution exactly equals the charge on the metal, and the charge on the metal is the net electroststic image charge (all the water molecules have electrostatic images but their net charge is zero).

C. Model for water and ions.

In all the calculations reported here we use the parameters of the Stillinger [5, 6] ST2 water model and the interaction parameters for alkali metal ions and water developed by Heinzinger and co-workers [7]. The ST2 water molecule model consists of a central oxygen atom (O_ST2 or O for short) surrounded by two hydrogen atoms (H_st2 or H for short) and two massless point charges (PC_ST2 or PC for short) in a rigid tetrahedral arrangement. The O-H and O-PC bond lengths were 0.10 nm and 0.08 nm respectively. This small difference in bond lengths means that the water_st2 model and its electrostatic image behave similarly. The only Lennard-Jones 'atom' in the ST2 model is the oxygen atom. The hydrogen H_ST2 and point charges PC_ST2 interact with their surroundings (i.e. other atoms and surfaces) only via Coulomb interactions. Their charges are q_H=0.23570|e| and q_{PC}=-q_H. The O atom has zero charge. The lithium ion was treated as a non-polarizable Lennard-Jones atom with point mass and charge. For example the (ε,σ) pairs are (0.3164, 0.3100) and (0.1490, 0.2370) for O_ST2 and Li ion respectively. The

units are ε in kJ/mole and σ in nm . The Lorentz-Berthelot combining rules were enforced for unlike species, namely: $\varepsilon_{AB} = (\varepsilon_{AA}\varepsilon_{BB})^{1/2}$ and $\sigma_{AB} = \frac{1}{2}(\sigma_{AA} + \sigma_{BB})$. The Stillinger switching function was used to modify the coulomb interactions between water molecules at close range. ends All molecule-molecule Lennard-Jones type interactions were cut-off in a smooth fashion at a molecular separation $R = 0.68$ nm.

D. Interaction between water and ions and the walls.

The metal was represented by two linearly superimposed potentials. Pauli repulsion and dispersive attractive interactions were represented by a 9-3 potential, and the interaction with the conduction electrons by an electroststic image potential. In the calculations described here the image plane and origin plane of the 9-3 potential were chosen coincident. This was tantamount to choosing the image plane and the nuclear plane of the metal surface to be same plane. This is acceptable in our scheme because the Lennard-Jones core parameters σ are all large and the 'thickness' of the repulsive wall is also large (ca. 0.247 nm). The atom-surface interaction parameters describing interaction with nonconduction electrons were chosen to be the same as those used by Lee at al [8], The well depth is approximately equal to thermal energy 'kT' or about 2.4 kJ/mole.

G. Electrostatics

During the molecular dynamics simulations the fast multipole method developed by Greengard and Rokhlin [9-12] was used to evaluate all long range sums of electrostatic interactions without truncation. The charge on the electrode is the image charge -lel. At any instant during the molecular dynamics run, this charge is not uniformly distributed across the electrode but localized on the surface in such a way as to produce the same electric field and potential as the electrostatic image of the lithium ion and all the water molecules. The field acting on the lithium ion comes from all the water molecules in the cell, all water and ions in the xy periodical replicant cells, and all of the electrostatic images of the contents of all cells in the image plane of the metal. We emphasize again that in this calculation as in all the others described in this paper no electrostatic interaction is truncated.

There are two useful ways to calculate the average time independent electric potentials from stored molecular dynamics trajectories. The reason for doing this is to make comparisons with averaged potentials calculated by other theories, e.g., Gouy-Chapman. The first method (the atom approach) uses the charge or partial charge on each atom and the three space coordinates of each atom recorded at regular time separations (usually 1 ps) as input into the generation of a charged source distribution. The source term for Maxwell's equations is the charge density function in vacuum. Without any local spatial averaging this point of view is similar to that followed by Wilson, Pohorille, and Pratt[13, 14]. The second way (the molecule method) views the dynamical system as a collection of molecules with internal electrical structure. These are inherently more complex objects than atoms. To specify the electrical properties we need the space coordinates, orientations and electrostatic multipole moments of each ion and molecule in the system. The approach we follow was described by Russakoff[15]. This derivation of a set

of macroscopic Maxwell equations from the equations of charged particles in vacuum is summarized in a number of standard texts[16]. We note that though the dynamics are uniquely defined by the models we use, the time independent average fields and potentials that are calculated are not unique because we can broaden the point charge distributions inside the ions and molecules in a spherically symmetric way and so long as the broaden distributions stay well inside the Lennard-Jones spheres (so that distributions on different molecules do not overlap) the the dynamics are unchanged. This means we can smooth some of the averages within limits set by geometry of the models and the energetics of collisions. This point has already been pointed out by Wilson, Pohorille and Pratt[13, 17] in their interesting discussion of the properties of the vacuum-water surface.

The atom method uses the distribution of point charges in vacuum. Consider the set of point charges without regard for whether they originate from neutral water molecules or charged ions. In this case the source term for Maxwell fields in vacuum is the microscopic charge density

$$\rho_I(\mathbf{r},t) = \rho_{metal}(\mathbf{r},t) + \rho_{atoms}(\mathbf{r},t). \qquad [2.2]$$

where

$$\rho_{metal}(\mathbf{r},t) = \rho_{metal}(x,y,t)\delta(z - \tfrac{1}{2}L), \qquad [2.3]$$

and

$$\rho_{atoms}(\mathbf{r},t) = \sum_{j=1}^{N_{atoms}} q_j \delta[\mathbf{r} - \mathbf{r}_j(t)], \qquad [2.4]$$

Here N_{atoms} is the number of atoms in the simulation cell and $\mathbf{r}_j$ is the position of the j-th atom. The surface charge density on the metal $\rho_{metal}(x,y,t)$ is time dependent because it depends on the position of the atomic charges. All the charge in the system is described by ρ_I. We can subject this charge density to local space averaging using a test function. Let $f(\mathbf{r})$ be a real positive function localized around $\mathbf{r} = 0$. We define the local spatial average of $F(\mathbf{r}, t)$ by

$$\langle F(\mathbf{r}, t)\rangle = \int d\mathbf{r}'\, f(\mathbf{r}')F(\mathbf{r} - \mathbf{r}', t). \qquad [2.5]$$

The time average can be replaced by an average over configurations at different times

$$\bar{F}(\mathbf{r}) = \lim_{t \to \infty} \frac{1}{t}\int_0^t dt' \langle F(\mathbf{r}, t')\rangle \approx \frac{1}{N_{configs}} \sum_{i=1}^{N_{configs}} \langle F(\mathbf{r}, t_i)\rangle. \qquad [2.6]$$

The system has translational invariance in the xy plane therefore $\overline{F}(\mathbf{r})$ is only a function of z. Consequently we consider only test functions $f(z)$ like the localized one dimensional Gaussian function

$$f(z) = (\pi g^2)^{-1/2}\, e^{-(z/g)^2}. \qquad [2.7]$$

We will subsequently refer to g as the gaussian width or 'bin' width. The metal surface charge density $\rho_{metal}(x,y,t)$ is replaced by the averaged image charge density which is a constant. The metal image charge is denoted by $\overline{\rho}_{metal}$. After the configurational averages are performed we get the z dependent charge density

$$\overline{\rho}_I(z) = \overline{\rho}_{metal}\delta(z - \tfrac{1}{2}L) + \overline{\rho}_{atoms}(z) \qquad [2.8]$$

where after substituting explicitly for the test function we get

$$\overline{\rho}_{atoms}(z) = \frac{1}{N_{configs}} \sum_{i=1}^{N_{configs}} \sum_{j=1}^{N_{atoms}} q_j f[z - z_j(t_i)]. \qquad [2.9]$$

The electric field and potential are given by integrating the vacuum Maxwell's equation over the remaining space variable z

$$\overline{E}_{I,z}(z) = \frac{1}{\varepsilon_0}\int_{-\infty}^{z} dz'\, \overline{\rho}_I(z') \quad , \qquad \overline{\Phi}_I(z) = -\frac{1}{\varepsilon_0}\int_{-\infty}^{z} dz' \overline{E}_{I,z}(z'). \qquad [2.10]$$

The second approach treats the system as a collection of molecules (labels n, positions $\mathbf{r}_n$) composed of atoms (label b, position $\mathbf{r}_{nb}$, charge q_{nb}). The charge density of the system is still the same as $\rho_I(\mathbf{r}, t)$ but with the atoms collected into molecular groups. For the molecule method we write the charge density as follows:

$$\rho_{II}(\mathbf{r},t) = \rho_{metal}(x,y,t)\delta(z - \tfrac{1}{2}L) + \rho_{mol}(\mathbf{r},t) \qquad [2.11]$$

where ρ_{metal} is the same charge density on the metal surface as in the atomic method, and the charge density from the molecules is

$$\rho_{mol}(\mathbf{r},t) = \sum_{n=1}^{N_{mol}} \rho_n(\mathbf{r},t) \;=\; \sum_{n=1}^{N_{mol}} \sum_{b=1}^{N_{na}} q_{nb}\delta[\mathbf{r} - \mathbf{r}_n(t) - \mathbf{r}_{nb}(t)], \qquad [2.12]$$

Here N_{mol} is the total number of molecules in the system, The number of atoms in the n th molecule is N_{na}, and $\mathbf{r}_{nb}$ is the position of the charge q_{nb} measured from the center $\mathbf{r}_n$ of the n th molecule. Note that $\mathbf{r}_n$ and $\mathbf{r}_{nb}$ are time dependent.

Next we perform explicit local spatial averaging with a test function and take the ensemble average. These steps are formally the same as described for the atom method. Then for each molecule (label n) we take the average with respect to the test function $f(z)$, and make a Taylor expansion of atomic coordinates $\mathbf{r}_{nb}$ relative to the molecular centers $\mathbf{r}_m$. This yields the following expression for the averaged charge density by the molecule method

$$\overline{\rho}_{mol}(z) = \overline{\rho}(z) - \frac{d}{dz}\overline{P}_z(z) + \frac{d^2}{dz^2}\overline{Q}_{zz}(z) - \frac{d^3}{dz^3}\overline{O}_{zzz}(z) + \cdots \qquad [2.13]$$

where

$$\overline{\rho}(z) = \frac{1}{N_{configs}} \sum_{i=1}^{N_{configs}} \sum_{m=1}^{N_{mol}} f[z - z_m(t_i)\,] \sum_{b=1}^{N_{ma}} q_{mb} \qquad [2.14]$$

$$\overline{P}_z(z) = \frac{1}{N_{configs}} \sum_{i=1}^{N_{configs}} \sum_{m=1}^{N_{mol}} f[z - z_m(t_i)\,] \sum_{b=1}^{N_{ma}} q_{mb} z_{mb}(t_i) \qquad [2.15]$$

$$\overline{Q}_{zz}(z) = \frac{1}{N_{configs}} \sum_{i=1}^{N_{configs}} \tfrac{1}{2} \sum_{m=1}^{N_{mol}} f[z - z_m(t_i)\,] \sum_{b=1}^{N_{mb}} q_{mb} z_{mb}(t_i) z_{mb}(t_i) \qquad [2.16]$$

$$\overline{O}_{zzz}(z) = \frac{1}{N_{configs}} \sum_{i=1}^{N_{configs}} \frac{1}{6} \sum_{m=1}^{N_{mol}} f[z - z_m(t_i)\,] \sum_{b=1}^{N_{mb}} q_{mb} z_{mb}(t_i) z_{mb}(t_i) z_{mb}(t_i) \qquad [2.17]$$

Here the charge density in the second method has been resolved into contributions from monopoles (ions only in this paper), dipoles, quadrupoles, octopoles, and higher order terms (all from the solvent in this paper).

III. SINGLE METAL ION

In this section we first describe briefly the probability density distribution calculated from molecular dynamics trajectories. Then we discuss the contibutions that the electrostatic multipoles make to the total electric potential. Finally we discuss the sensitivity of the potential and its components to the width of the test function used in the calculation.

The simulation was run for 2000 ps, the first 100 ps of which were used to equilibrate the system. Figure 2 shows the probability density profiles for the atoms, ions and water averaged over the xy plane. Also shown at top in Figure 2 is the electrical potential calculated by the atom method using a gaussian test function with a width of g = 0.03 nm. It is shown with the probability distributions to highlight features due to water the majority species. Note that in Figure 2 the scale for water and its components differ from the lithium ion by a factor of fifty.

In Figure 2 the Li^+ ion mass center maps out a diffuse-like region between -0.6 and 0.4 nm. The small ionic radius of Li^+ ensures that its primary solvation shell is tightly bound making it the core of a much larger composite object. Only in a particularly high surface electric field can this object dissociate and permit the Li^+ cation to contact adsorb on the electrode. The apparent asymmetry of the distribution may be due to the limited width of the cell and consequently no significance is attached to its shape other than it is diffuse in nature. The ion can be pulled closer to the metal by applying an external uncompensated electric field. Uncompensated field cannot be screened completely by ions present in the solution. This is convenient way to check the sensitivity of an ion to adsorption in higher fields, without having to resort to a separate lengthy computer simulation. When the surface field was roughly equal to that produced by doubling the negative charge on the metal, the lithium ion did not contact adsorb[18, 19], whereas all the larger cat ions (Na^+, K^+, Rb^+, and Cs^+) did contact adsorb.

To check for large effects due to correlated motion between two Li^+ ions in the same simulation cell we performed the calculations for several hundred picoseconds with a system about four times larger (two lithium ions and 598 water molecules). The water density profiles when appropriately scaled appeared almost exactly the same, and the lithium probability $\rho(z)$ profile was again spread across the cell and formed a diffuse zone with a moderate bias toward the metal. This latter result provides some reassurance that small simulations can give usefully information about water structure within two or three layers from the surface.

Near the metal the ion center did not pass z = 0.4 nm. This meant it was never closer than 0.3 nm to the point where the wall potential passed through zero (vertical dashed line at 0.6 nm in Figure 2). At this point of closest approach there is still room for one water molecule between the ion and the metal. In Grahame's picture of aqueous electric double layers[3, 4] water in the primary solvation shell of small ions can touch the electrode surface. In contrast in the model proposed by Bockris[1, 3] the solvated ion does not displace water in the first layer next to the charged metal, and the ion is always at a distance of about two water molecules from the surface. In the simulations described here the ion behaved like the picture due to Grahame. A more detailed model of adsorption in which the ion interacts with atoms and electrons comprising the surface is beyound the scope of the present work. In passing we mention that metal-water po-

tentials exist for platinum and several other metals. Generally the effective well depths are large and to calculate distribution profiles requires either very long simulation times (> 10 ns) and or the use of specialized sampling techiques[20].

The water profile shows some new structure not seen in water without ions[19, 21]. Most interesting is the peak closest to the metal surface at ca. 0.68 nm due to a few localized water molecules. The orientation of these localized water molecules can be determined from the H_ST2 and PC_ST2 probability distributions. The protons on these molecules give rise the distinct peak at ca. 0.75 nm in the H_ST2 distribution. In the PC_ST2 distribution there is peak at ca. 0.625 nm that is enhanced more than the second peak in the H_ST2 profile at ca. 0.6 nm. The first water peak at ca. 0.68 nm lies between the first H and PC peaks measured from the metal surface. The positions and relative intensities of these peaks suggests that some of the localized water molecules have one proton pointing at the electrode. This would permit the system to adopt an ice-like configuration with hydrogen bonding to a second layer of water, similar to that discussed by Lee et al[8]. We do not preclude other waters with two protons pointing at the surface these would have a dipole normal to the surface which is favored on the basis of simple electrostatics.

Figure 3 shows the electric potential (atom x10) across the cell calculated by the atomic charge method with a test function with gaussian width g = 0.03 nm. Also shown are the components of the electric potential coming from the ions (monopoles) and the point dipoles of the waters molecules. The component potentials were calculated by the molecular method. The components are monopole (mono), dipole, and monopole + dipole combined (m+d x10). Note that for $|z| < 0.6$ nm the monopole and dipole terms almost cancel.

The monopole contribution (mono in Figure 3) due to lithium ion alone drops monotonically as expected for the potential inside a capacitor where the charge on the left is in a diffuse layer spatially separate from the charge on the right plate (metal) at z = 0.931 nm. Adding the dipole completely changes the potential (see m+d x10 curve). The water molecules very effectively screen the field inside the capacitor, except for the region z > 0.68 nm where the water distribution drops rapidly to zero. The peak in m+d near 0.7 nm occurs where they no longer cancel and the monopole charge dominates.

Figure 4 shows some of the higher order electrostatic components of the electric potential. Quadrupole and octopole potentials are from the water molecules. To allow an easy comparison the monopole + dipole combined (m+d) potential is also plotted. Note that the quadrupole potential is approximately constant across the cell except near the metal where the potential has a sharp peak. The octopole potential is everywhere approximately zero except near the metal surface. Adding the quadrupole (also from water only) term brings the atomic and molecular calculations into some measure of agreement The quadrupole contribution to the potential is a negative constant in the region away from the wall potential. This occurs because its contribution to the charge $\langle \rho_{mol}(\mathbf{r},t) \rangle$ contains a double derivative in space coordinates. The differences are greatest at the surfaces where the atomic method traces charge density smoothly whereas the molecular method, based on an expansion about molecular centers, requires many high multi-

poles to describe the field. The dangers of omitting higher multipole were clearly pointed out by Wilson, Pororille and Pratt[13, 17] for water without ions.

We close this section with a discussion of changing the length scale over which the test function averaging is performed. The lithium system was chosen because prior work[18, 19] and systematic electrochemical experiments[2] has shown that small ions like lithium or fluoride form diffuse screening zones near charged electrodes, and have little tendency to contact adsorb. In Figure 5 shows the relative insensitivity of the monopole and dipole potentials to a change in the gaussian bin widths for the range g = 0.03 to 0.3 nm. The solid curves are for g = 0.03 nm and the broken curves for g = 0.3 nm. The smearing of monopole (ion) charge for g = 0.03 to 0.3 nm did not cause it to overlap the metal so that this component of the electric potential hardly changed. The dipole potential changed most with g, notably for z > 0.68 nm since the water density extended all the way to the repulsive region of the wall potential of the metal. Since the monopole and dipole potential almost cancel in the solution phase this makes the m+d potential sensitive to the detailed behaviour of the dipole near the surface.

Figure 6 shows the sensitivity of higher order electrostatic multipole potentials to gaussian bin widths for the range g = 0.03 to 0.3 nm. Solid curve for g = 0.03 nm, long broken curve for g = 0.1 nm, and short broken curve for g = 0.3 nm. The surface features of the quadrupole and octopole are washed out by the value g = 0.3 nm the size of the water molecule. Note that the quadrupole potential is averaged to a finite value, very roughly constant over the cell. The potential from the octopoles averages to zero over the whole cell for bin widths greater than g = 0.1 nm.

The effect of changing the gaussian width on the total potential is shown in Figures 7 and 8. In Figure 7 the sensitivity of the atom potential to the gaussian bin width is shown (solid curves) for g = 0.03 to 0.3 nm. The broken curves show the corresponding monopole potentials. The difference between the two sets of curves is due to the water. Note that the peak in the potential near 0.8 nm is completely washed out at g = 0.3 nm. Figure 8 shows a detail of Figure 7 in the range of small electric potentials (-.05 to .05). The gaussian bin widths are the same as before g = 0.03 to 0.3 nm. The corresponding monopole potentials are plotted for reference. Note that the peak in the potential near 0.75 nm is completely washed out by g = 0.3 nm.

Figures 7 and 8 demonstrate that as the size of the bin is increased from g = 0.03 nm (.1 x water molecule dimension) to g = 1.0 nm (3 x water molecule dimension) the structure in the electric potential near the surface due to the water profile is lost. The total potential becomes monotonic and resembles the shape of the monopole potential curves calculated using the monopole charge distribution. Since the component of the water dipole perpendicular to the surface is not averaged to zero the atom potential at the surface always remains smaller in magnitude than the monopole potential. We can regard this as an expression of dipole dielectric polarization which remains after gaussian averaging and reduces the value of the surface potential by roughly an order of magnitude (curves for g = .3 nm). As expected the monopole potentials are not as sensitive to the value of the width g as the atomic potentials. This is an interesting qualitative result because it shows the transition from the microscopic scale, where surface water oscillatory

structure dominates the potential, to macroscopic scale behaviour where water contributes simple scaling of the electric potential.

IV. CONCLUSIONS

For a system with non contact adsorbing cation we have used two methods to calculate a time independent electric potential from atom trajectories generated by a constant (N,V,T) molecular dynamics simulation. A key feature of the simulation was the calculation of all long range coulomb interactions including all electric image interactions without truncation. Each method provides some insight into the components of the potential contributed by the ion and the water molecules and the sensitivity of the multipole fields to the scale over which spatial averages were performed. The variation in potential near the metal was due to partially oriented water molecules. The importance of water dipole, quadrupole and octopole potentials was highlighted. Quadrupoles contribute roughly a constant value to the potential in the bulk and oscillatory structure near the surface. A significant contribution from octopoles and higher order multipoles occured near the surface where the fields are strong and the potential rapidly varying. The insensitivity of monopole and dipole to the spatial bin width was in contrast to the behaviour of the quadrupole and octopole.

ACKNOWLEDGEMENTS

This research was supported in part by the Office of Naval Research. The contributions of JNG were performed under the auspices of US DOE contract W-7405-Eng-48.

REFERENCES

1 J. O. Brockris, M. A. Devanathan, and K. Müller, Proc. Roy. Soc.(London) **A274**, 55-79 (1963.).

2 J. O. Bockris and A. K. Reddy, *Modern Electrochemistry, Vol.2* (Plenum Press, New York, 1973).

3 E. Gileadi, E. Kirowa-Eisner, and J. Penciner, *Interfacial Electrochemistry* (Addison-Wesley, Reading, Massachusetts, 1975).

4 D. C. Grahame., Chem. Rev. **41**, 441 - 501 (1947).

5 F. H. Stillinger and A. Rahman, J. Chem. Phys. **60**, 1545-1557 (1974).

6 O. Steinhauser, Mol. Phys. **45**, 335-348 (1982).

7 K. Heinzinger, in *Computer Modeling of Fluids Polymers and Solids,*, edited by C. R. A. Catlow, S. C. Parker, and M. P. Allen (Kluwer, Holland, 1990), Vol. 293, NATO ASI Series C, pp. 357-404.

8 C. Y. Lee, J. A. McCammon, and P. J. Rossky, J. Chem. Phys. **80**, 4448-4455 (1984).

9 L. F. Greengard, *The Rapid Evaluation of Potential Fields in Particle Systems.* (The MIT Press, Cambridge, Massachusetts, 1987).

10 L. Greengard and V. Rokhlin, J. Comp. Phys. **73**, 325-348 (1987).

11 J. Carrier, L. Greengard, and V. Rokhlin, Siam J. Sci. Stat. Comput. **9**, 669-686 (1988).

12 L. Greengard and V. Rokhlin, Chemica Scripta **29A**, 139-144 (1989).

13 M. A. Wilson, A. Pohorille, and L. R. Pratt, J. Chem. Phys. **88**, 3281 - 3285 (1988).

14 M. A. Wilson, A. Pohorille, and L. R. Pratt, Chem. Phys. **129**, 209 - 212 (1989).

15 G. Russakoff, Amer. J. Phys. **38**, 1188-1195 (1970).

16 J. D. Jackson, *Classical Electrodynamics* (Wiley, New York, 1975), pp. 54-62.

17 M. A. Wilson, A. Pohorille, and L. R. Pratt, J. Chem. Phys. **90**, 5211 - 5213 (1989).

18 J. N. Glosli and M. R. Philpott, J. Chem. Phys. **96**, 6962-6969 (1992).

19 J. N. Glosli and M. R. Philpott, J. Chem. Phys. **98**, 9995-10008 (1993).

20 D. A. Rose and I. Benjamin, J. Chem. Phys. **95**, 6856-6865 (1991).

21 M. R. Philpott and J. N. Glosli, in *Theoretical and Computational Approaches to Interface Phenomena*, edited by H. Sellers and J. T. Golab (Plenum, New York, 1994), pp. 75 - 100.

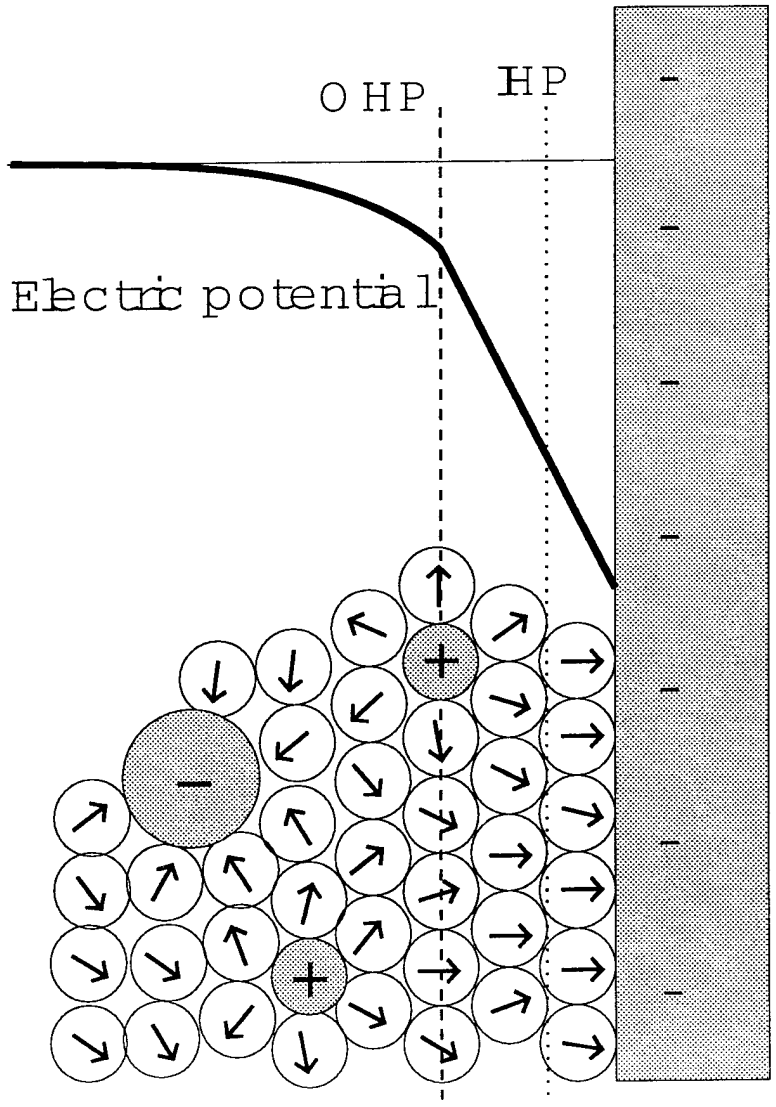

Figure 1. Schematic diagram of the charged metal electrode aqueous electrolyte interface. The metal is shown as a flat negatively charged surface and there is a fully hydrated cation at the outer Helmholtz plane (OHP) two water molecules distant. The top part shows a schematic of the electric potential assuming the ions are point charges in a dielectric continuum restricted to the solution side of the OHP.

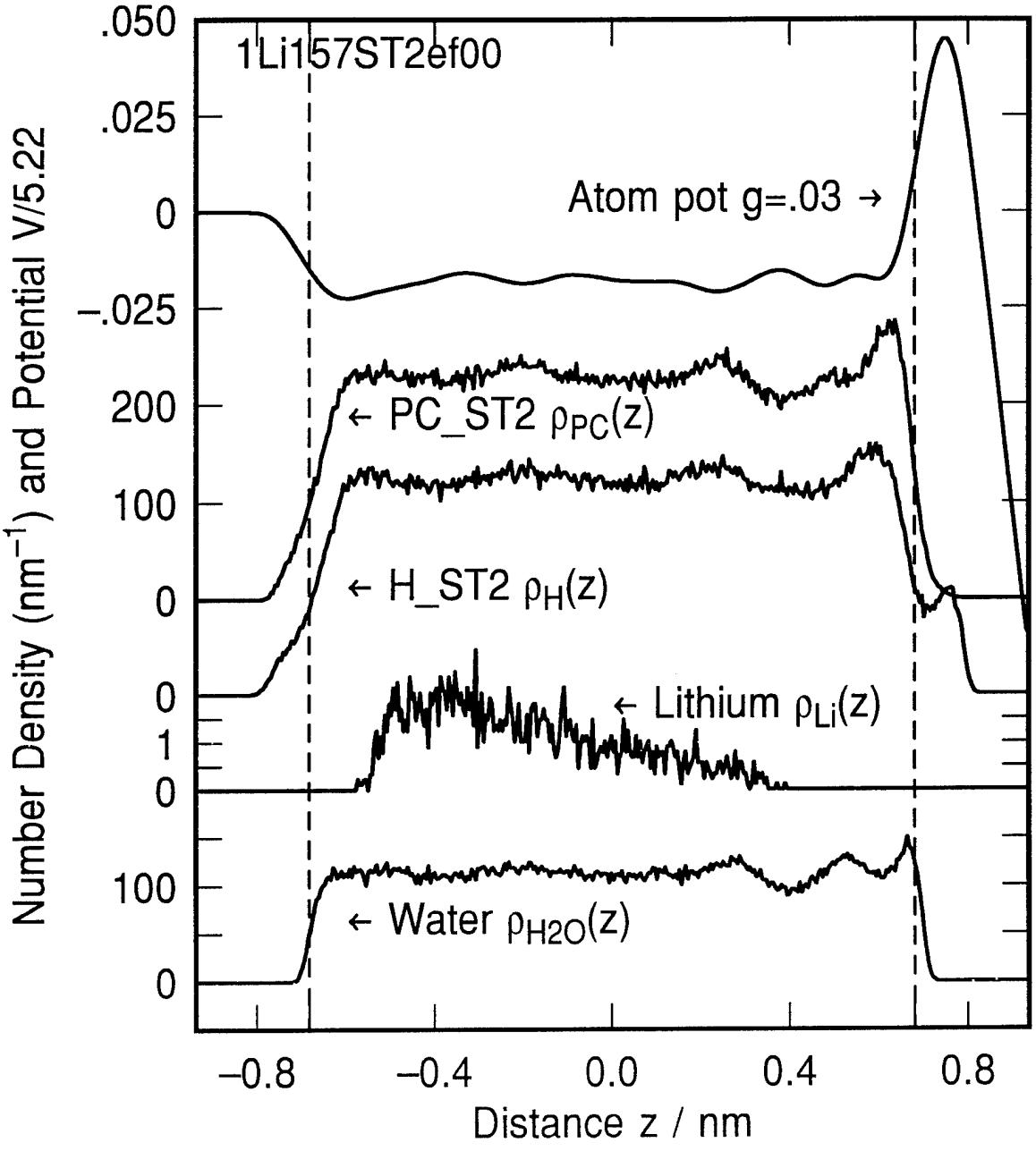

Figure 2. Electric potential and density profiles for lithium cation Li^+ ion and 157 STst2 waters near an immersed electrode. Metal electrode on right hand side, dielectric on the left. Image plane at z = 0.931 nm and wall potentials go through zero at |z| = 0.68 nm.

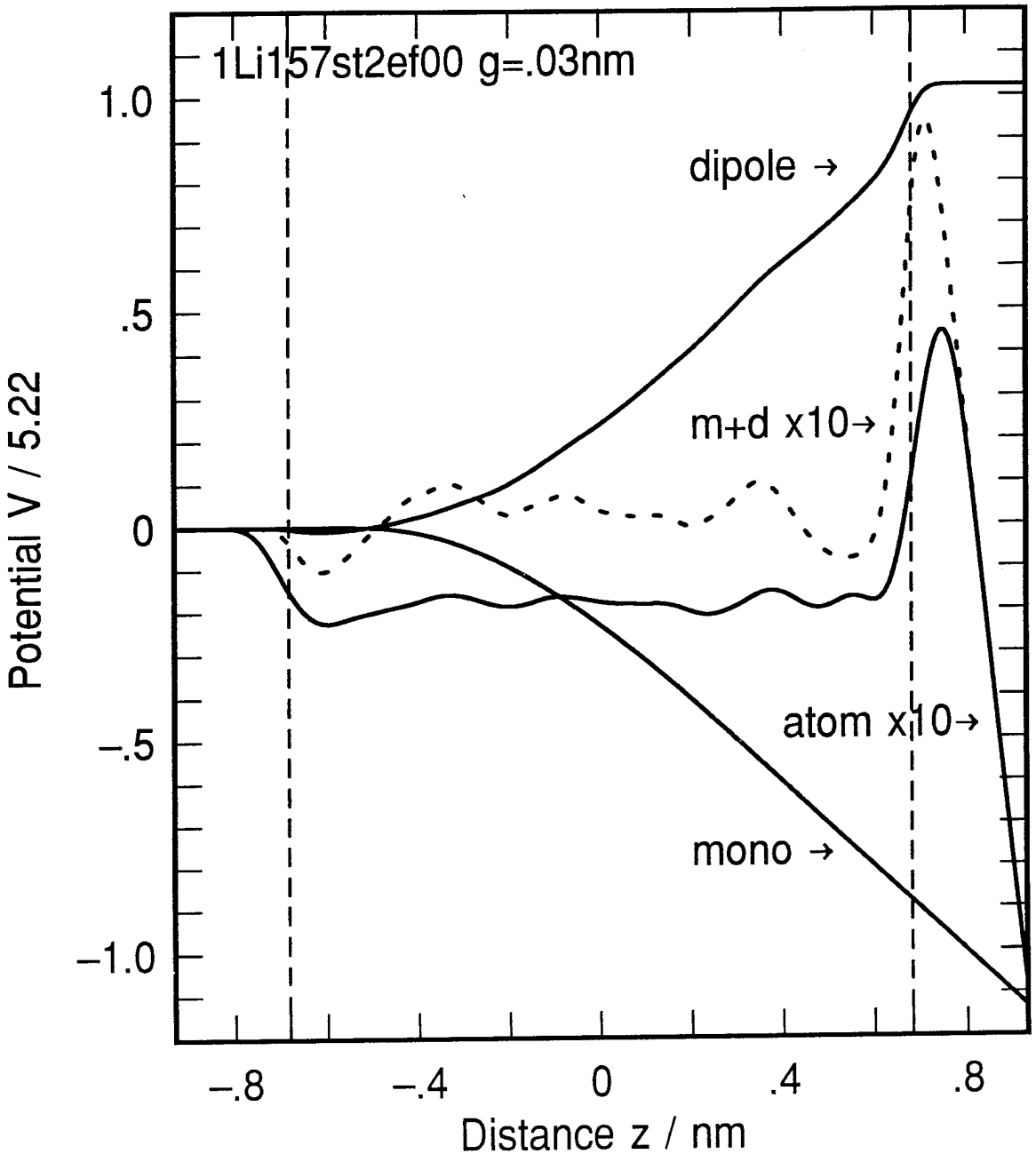

Figure 3. Electric potential (atom x10) and components of the potential calculated by the molecular method. The components are monopole (mono), dipole, and monopole + dipole combined (m+d x10). Note that for $|z| < 0.6$ nm the monopole and dipole terms almost cancel. Simulation cell contains one Li^+ ion and 157 st2 waters with the metal electrode on right hand side, and dielectric on the left. Image plane at z = 0.931 nm and wall potentials go through zero at $|z|$=0.682 nm.

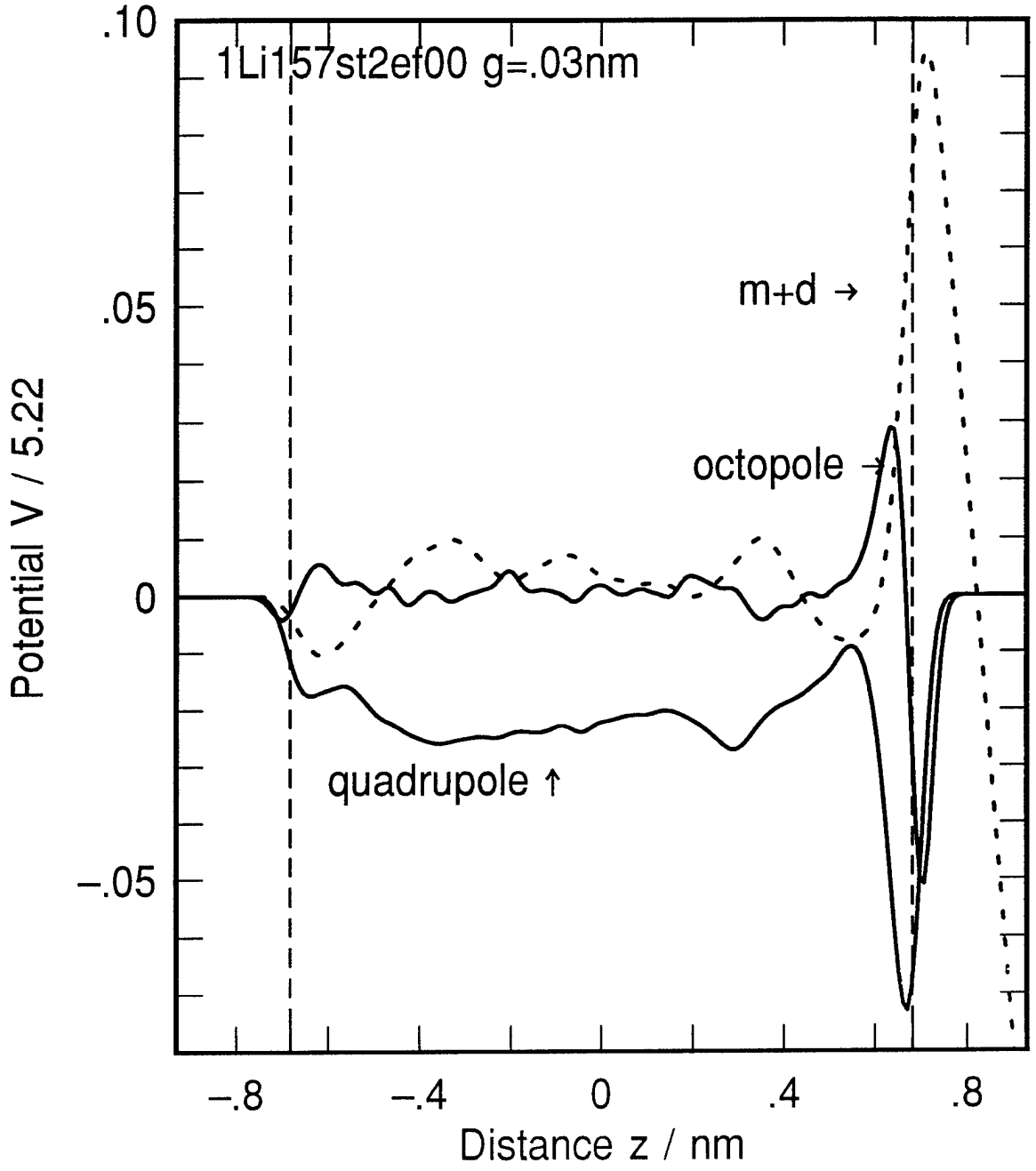

Figure 4. Higher order electrostatic components of the electric potential. Quadrupole and octopole potentials from the water molecules. For comparison the monopole + dipole combined (m+d) potential is also plotted. Note that the quadrupole potential is approximately constant across the cell except near the metal where the potential has a sharp peak. The octopole potential is everywhere approximately zero except near the metal surface. Simulation cell contains one Li^+ ion and 157 st2 waters with the metal electrode on right hand side, and dielectric on the left. Image plane at z = 0.931 nm and wall potentials go through zero at |z|=0.682 nm.

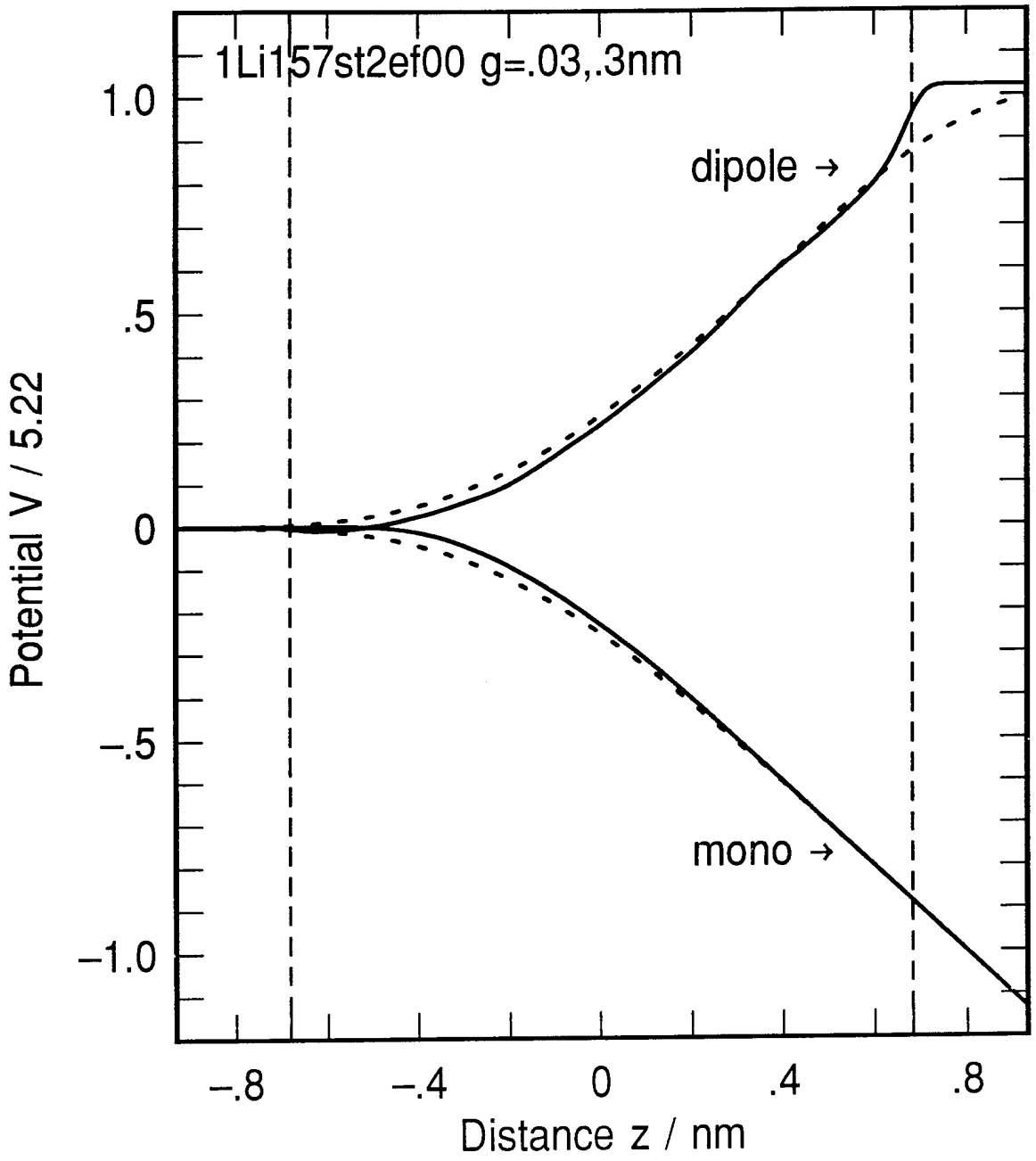

Figure 5. Insensitivity of low order electrostatic multipole potentials to gaussian bin widths for the range g = 0.03 to 0.3 nm. Solid line result for g = 0.03 nm, broken line result for g = 0.3 nm. Monopole and dipole do not change value except the dipole for z > 0.68 nm where the water density is very small. Simulation cell contains one Li^+ ion and 157 st2 waters with the metal electrode on right hand side, and dielectric on the left. Image plane at z = 0.931 nm and wall potentials go through zero at |z|=0.682 nm.

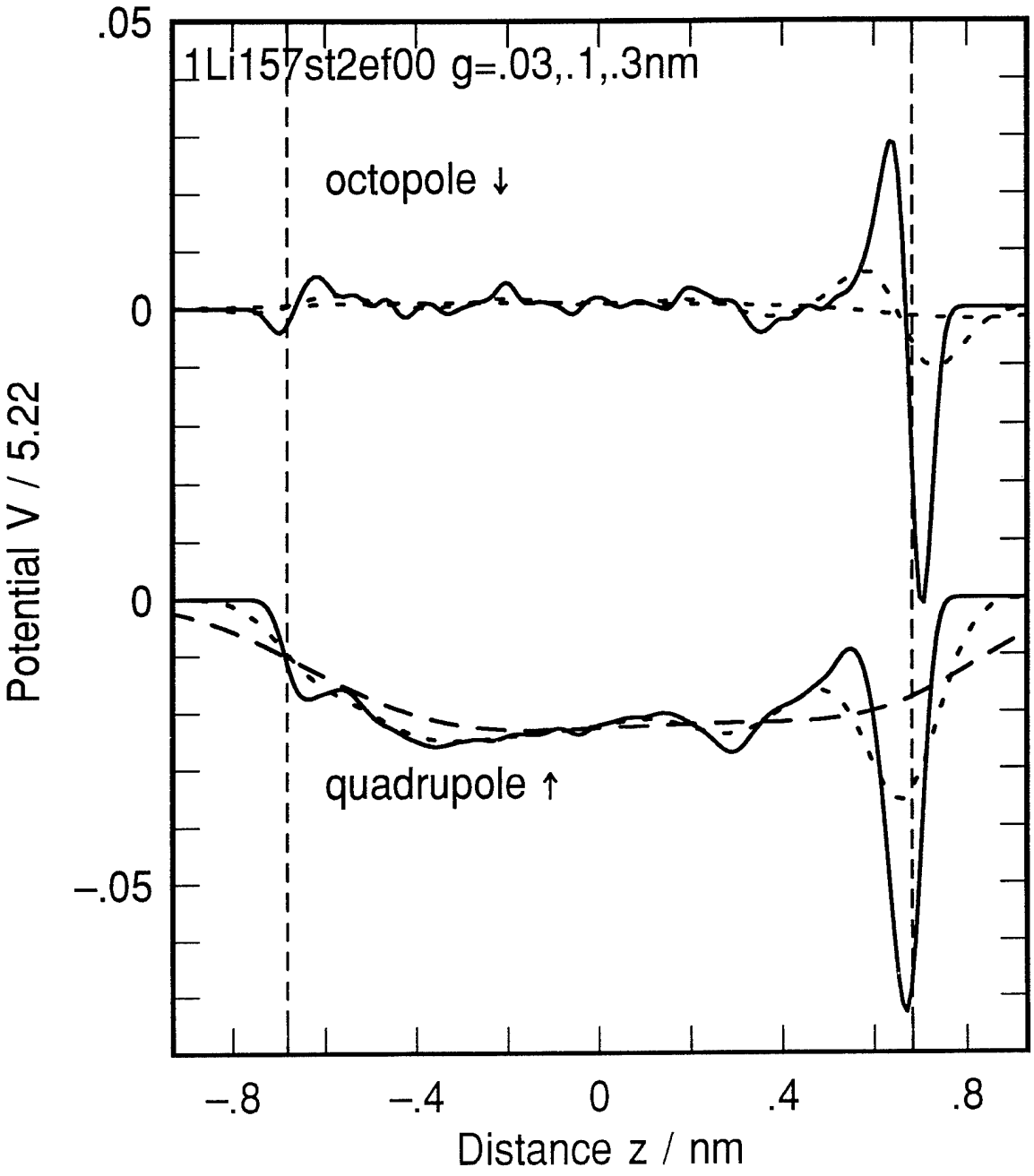

Figure 6. Sensitivity of higher order electrostatic multipole potentials to gaussian bin widths for the range g = 0.03 to 0.3 nm. Note that the quadrupole loses the surface peak for a width equal to the water molecule dimension 0.3 nm. The octopole potential averages to zero over the whole cell. Simulation cell contains one Li^+ ion and 157 st2 waters with the metal electrode on right hand side, and dielectric on the left. Image plane at z = 0.931 nm and wall potentials go through zero at |z|=0.682 nm.

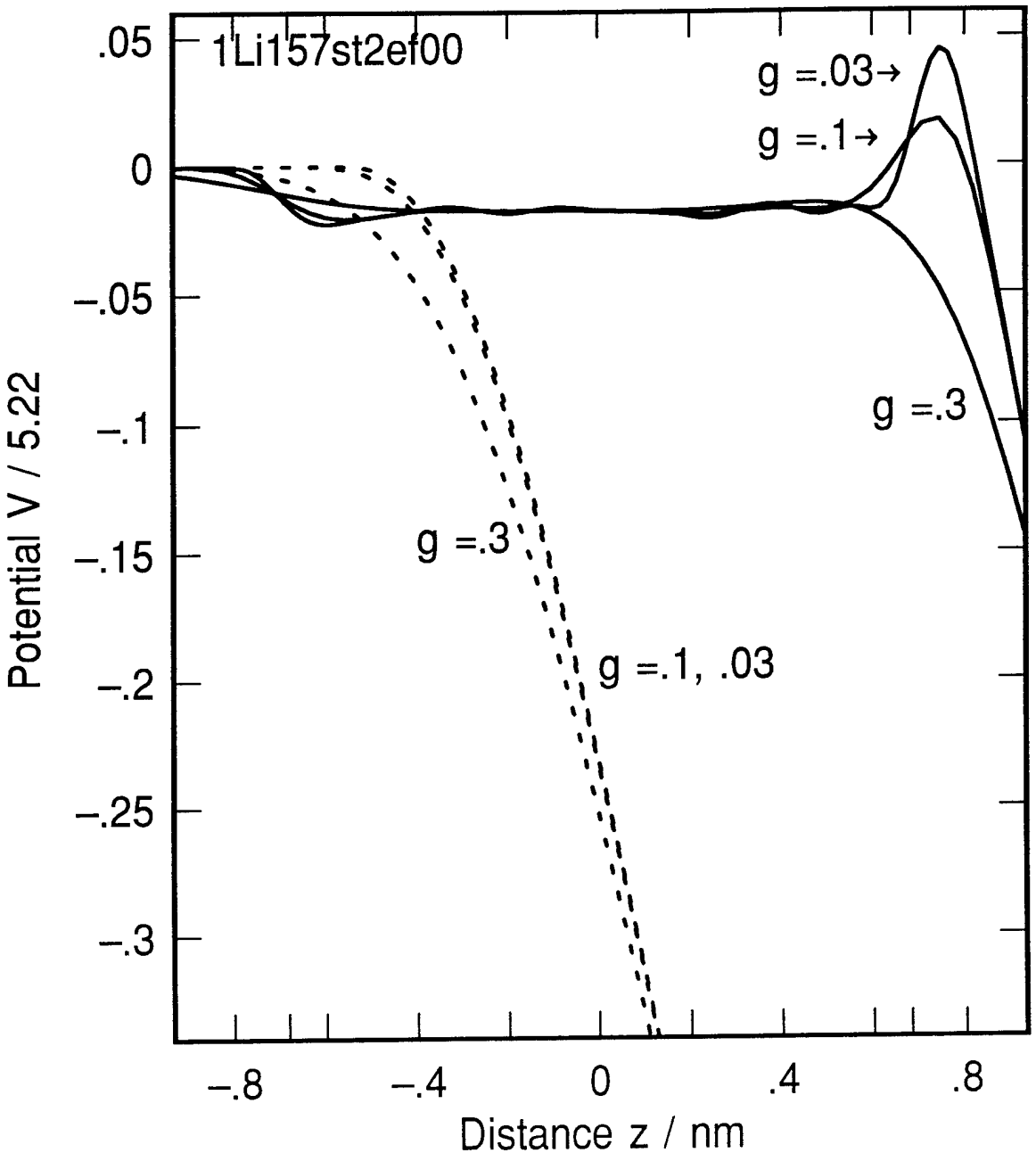

Figure 7. Sensitivity of the atom method electric potential to to gaussian bin widths for the range g = 0.03 to 0.3 nm. The corresponding monopole potentials are plotted for reference. Note that the peak in the potential near 0.8 nm is completely washed out at g = 0.3 nm. Simulation cell contains one Li^+ ion and 157 st2 waters with the metal electrode on right hand side, and dielectric on the left. Image plane at z = 0.931 nm and wall potentials go through zero at |z|=0.682 nm.

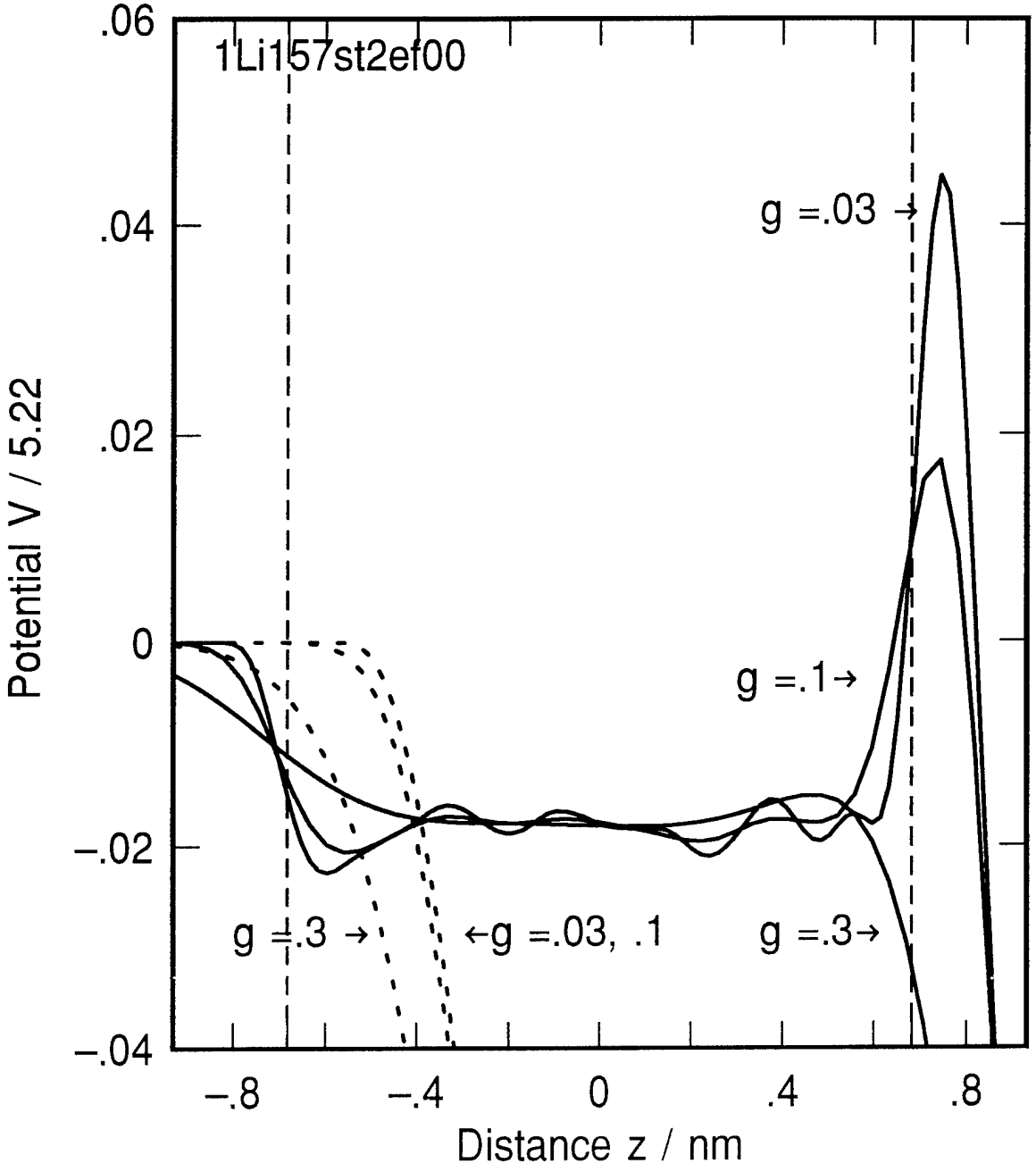

Figure 8. Detail showing the small potential range (< .05) of the sensitivity of the atom method electric potential to to gaussian bin widths for the range g = 0.03 to 0.3 nm. The corresponding monopole potentials are plotted for reference. Note that the peak in the potential near 0.8 nm is completely washed out at g = 0.3 nm. Simulation cell contains one Li^+ ion and 157 st2 waters with the metal electrode on right hand side, and dielectric on the left. Image plane at z = 0.931 nm and wall potentials go through zero at |z|=0.682 nm.